

# Formononetin suppresses the malignant progression of papillary thyroid carcinoma depending on downregulation of CBX4

HONGBO YU<sup>1</sup>, JI QU<sup>1</sup>, HAIXIN GOU<sup>1</sup> and YING ZHOU<sup>2</sup>

<sup>1</sup>Department of Traditional Chinese Medicine Traumatology and Surgery, Huadong Hospital Affiliated to Fudan University, Shanghai 200040; <sup>2</sup>Department of Vascular Medicine, Shanghai Traditional Chinese Medicine-Integrated Hospital Affiliated to Shanghai University of Traditional Chinese Medicine, Shanghai 200082, P.R. China

Received September 26, 2023; Accepted February 26, 2024

DOI: 10.3892/etm.2024.12746

**Abstract.** Papillary thyroid carcinoma (PTC) is the most common malignant tumor of the endocrine system globally. Formononetin (FMNT), an isoflavonoid, exerts anti-tumorigenic effects and chromobox homolog 4 (CBX4) exerts tumor-promoting effect in specific types of tumors. Nevertheless, the predictive values and biological functions of FMNT and CBX4 in the pathological progress of PTC have not been fully understood till now. In the present study, the human PTC cell line TPC-1 was exposed to 0, 10, 30 and 100  $\mu$ M FMNT for 24 h to elucidate the precise effects of FMNT on the biological behaviors of PTC cells. Moreover, FMNT-treated TPC-1 cells were transfected with oe-CBX4 to evaluate whether CBX4 was implicated in the anticarcinogenic effects of FMNT against PTC. It was demonstrated that FMNT treatment suppressed the proliferation, clone formation, migration, invasion, EMT, angiogenesis and stemness of PTC cells in a dose-dependent manner. Furthermore, it was verified that FMNT targeted CBX4 to downregulate its expression in a dose dependent manner. The suppressive effects of FMNT on the proliferation, clone formation, migration, invasion, EMT, angiogenesis and stemness of PTC cells were partially reversed by CBX4 overexpression. Upregulation of CBX4 abolished the tumor suppression effects of FMNT in the malignant progression of PTC. In conclusion, FMNT might act as a promising anti-tumorigenic agent in PTC, which depends on the downregulation of CBX4.

## Introduction

Thyroid cancer is the most common malignancy of the endocrine system worldwide, and its global incidence has been steadily rising in recent decades (1). Papillary thyroid carcinoma (PTC), the most frequent subtype of thyroid cancer, accounts for 80-85% of thyroid cancers in the population (2). The majority of patients with PTC respond well to existing therapeutic strategies, with a 10-year survival of >90% (3). Nevertheless, recurrence and distant metastasis have always been two major causes of death in PTC (4). Thus, there is an urgent need to thoroughly understand PTC pathogenesis and develop effective therapeutic strategies against the malignant progression of PTC.

Formononetin (FMNT; PubChem CID: 5280378), an isoflavonoid isolated from *Astragalus membranaceus* and *Spatholobus suberectus*, possesses numerous pharmacological effects, such as anti-inflammatory, anti-oxidant and anticancer properties (5). Previous studies have reported that FMNT can act as a novel anti-tumorigenic agent to induce cell growth inhibition and cell cycle arrest, promote cell apoptosis, inhibit metastasis and reduce angiogenesis in a panel of solid tumors including breast (6-8), colorectal (9), gastric (10) and lung cancer (11). A comprehensive grasp of cellular processes and molecular signaling pathways involved in FMNT-mediated antitumor activities is of great urgency.

Polycomb group (PcG) complexes, have been reported to act as epigenetic regulatory complexes and to be dysregulated in certain cancers, such as breast cancer, prostate cancer, and hepatocellular carcinoma, and to participate in tumorigenesis and tumor progression (12). The chromobox (CBX) family proteins, canonical components of PcG complexes, can regulate tumorigenesis and tumor progression by inhibiting the cell differentiation and self-renewal of cancer stem cells (13). CBX4, also known as polycomb 2, is both a SUMO E3 ligase and a transcriptional regulator involved in cell cycle regulation and DNA damage repair (14,15). Previous studies have described the tumor-promoting effect of CBX4 in malignant tumors, such as hepatocellular carcinoma (16), lung cancer (17), gastric cancer (18), clear cell renal cell carcinoma (19) and breast cancer (20). However, the prognostic value and biological function of CBX4 in the malignant progression of PTC remain unclear.

---

*Correspondence to:* Dr Ying Zhou, Department of Vascular Medicine, Shanghai Traditional Chinese Medicine-Integrated Hospital Affiliated to Shanghai University of Traditional Chinese Medicine, 230 Baoding Road, Hongkou, Shanghai 200082, P.R. China  
E-mail: zhouying820826@163.com

**Key words:** formononetin, chromobox homolog 4, papillary thyroid carcinoma

In the present study, the proliferation, clone formation, migration, invasion, EMT, angiogenesis and stemness of PTC cells were evaluated, so as to demonstrate the anti-tumorigenic effect of FMNT and the tumor-promoting effect of CBX4 in the malignant progression of PTC. Moreover, the study attempted to expound the association between FMNT and CBX4 and to identify the potential molecular mechanism.

## Materials and methods

**Cell culture.** The human PTC TPC-1 and normal human thyroid Nthy-ori3-1 cell lines were purchased from Cobioer Co., Ltd. TPC-1 cells were maintained in Dulbecco's modified Eagle's medium (Gibco; Thermo Fisher Scientific, Inc.) supplemented with 10% fetal bovine serum (FBS; Gibco; Thermo Fisher Scientific, Inc.) and 1% penicillin-streptomycin solution (MilliporeSigma) at 37°C in a humidified environment with 5% CO<sub>2</sub>. Nthy-ori3-1 cells were maintained in Roswell Park Memorial Institute-1640 medium (Gibco; Thermo Fisher Scientific, Inc.) supplemented with 10% FBS and 1% penicillin-streptomycin solution at 37°C in a humidified environment with 5% CO<sub>2</sub>.

**Cell treatment.** Nthy-ori3-1 cells and TPC-1 cells were exposed to 0, 10, 30 or, 100 μM FMNT for 24 h at 37°C.

**Cell transfection.** CBX4 overexpression plasmid (oe-CBX4) was established by inserting the CBX4 gene into a pcDNA3.1 vector (Shanghai GenePharma Co., Ltd.), whereas an empty vector served as the negative control (oe-NC). Cells were transfected, when they reached ~85% confluence with 5 μg/ml oe-CBX4 and oe-NC using Lipofectamine<sup>®</sup> 2000 (Invitrogen; Thermo Fisher Scientific, Inc.) at 37°C for 48 h strictly according to the manufacturer's guidelines. Cells were collected 48 h post transfection for use in subsequent experiments.

**Bioinformatics analysis.** CBX4 expression in thyroid cancer tissues was analyzed using the Encyclopedia of RNA Interactomes (ENCORI; <http://rna.sysu.edu.cn/encori/mirTar-Pathways.php>) database.

**Molecular docking.** The 3-D structure of CBX4 (PDB ID: 5EPL) was obtained from the protein data bank (PDB) database (<https://www.rcsb.org/>). Molecular docking was conducted using AutoDockTools 4.2 software (<https://autodock.scripps.edu/>) and the 3D diagrams of molecular docking models were visualized using PyMol software (version 3.0; <https://pymol.org/>).

**Cell Counting Kit-8 (CCK-8) assay.** The viability of TPC-1 or Nthy-ori3-1 cells was determined using the CCK-8 assay. The cells (5x10<sup>3</sup> cells/well) were inoculated into 96-well plates for 24 h of incubation and then exposed to 0, 10, 30 or, 100 μM FMNT for 24 h. 10 μl CCK-8 reagent (Beyotime Institute of Biotechnology) was added into each well for a further 4 h incubation at 37°C. The microplate reader (Bio-Rad Laboratories, Inc.) recorded the optical density at 450 nm.

**5-ethynyl-2'-deoxyuridine (EdU) staining.** The proliferation of TPC-1 cells was determined using the BeyoClick™ EdU

Cell Proliferation Kit (Beyotime Institute of Biotechnology) according to the manufacturer's protocol. The cells were incubated with EdU reagent for 2 h at 37°C, fixed in 4% paraformaldehyde for 15 min, permeabilized in 0.3% Triton X-100 for 10 min and subsequently incubated with the BeyoClick reaction solution in darkness for 30 min. Representative images of EdU-positive cells were captured using a fluorescence microscope (magnification, x200).

**Colony formation assay.** The clone-forming ability of TPC-1 cells was determined by employing colony formation assays. The cells were digested with 0.25% trypsin, resuspended in complete medium and inoculated (500 cells/well) into 6-well plates for further culture, and the medium was changed every two days. The cells were incubated for 14 days at 37°C, fixed with 4% paraformaldehyde at room temperature for 30 min and stained with 0.1% crystal violet at room temperature for 10 min. Images of visible colonies (≥50 cells) were captured using a digital camera (magnification, x1).

**Spheroid formation assay.** TPC-1 cells (5x10<sup>3</sup>/well) seeded in 6-well ultra-low attachment plates were maintained in serum-free medium supplemented with 20 ng/ml epidermal growth factor (EGF), 20 ng/ml basic fibroblast growth factor, 20 μl/ml B27 supplement and 1% penicillin-streptomycin in a humidified atmosphere of 5% CO<sub>2</sub> at 37°C. After incubation for 7-10 days, tumor spheroids (diameter >100 μm) were counted and image using a light microscope (magnification, x200).

**Wound healing assay.** The migratory capability of TPC-1 cells was assessed using a wound healing assay. The cells (1x10<sup>6</sup> cells/well) seeded in 6-well plates were cultured to ~95% confluence. A sterile 200-μl pipette tip was used to vertically scratch the cells to create the 'wound' and the detached cells were removed by washing twice with PBS. The cells were then supplemented with fresh serum-free medium for incubation for 24 h at 37°C. Images of the wound area at 0 and 24 h after wounding were captured using a light microscope (magnification, x100). The migration rate was calculated according to the width of the wounds measured using Image J software (version 1.52; National Institutes of Health).

**Transwell assay.** The invasive capability of TPC-1 cells was determined by employing Transwell assay. The cells were collected, resuspended in fresh serum-free medium and placed (2x10<sup>4</sup> cells/well) in the upper layer of Transwell chamber precoated with Matrigel at 37°C for 30 min. The lower layer of Transwell chamber was supplemented with the complete medium as a chemoattractant. After 24 h of incubation, invasive cells in the lower chamber were fixed with 4% paraformaldehyde at room temperature for 30 min, stained with 0.1% crystal violet at room temperature for 10 min, images were captured using a light microscope and the number of cells was quantified using Image J software (version 1.52; National Institutes of Health) (magnification, x100).

**Tube formation assay.** The conditioned media (CM) of TPC-1 cells was collected post 24-h incubation. Human umbilical vein endothelial cells (HUVECs) (2x10<sup>4</sup> cells/well; iCell-h110; Cellverse Bioscience Technology Co., Ltd.) seeded in 96-well

plates precoated with Matrigel at 37°C for 30 min were cultured in CM for 24 h and images of tube formation were captured using a light microscope (magnification, x200).

**Reverse transcription-quantitative polymerase chain reaction (RT-qPCR).** Total RNA was extracted from TPC-1 cells using TRIzol<sup>®</sup> reagent (Invitrogen; Thermo Fisher Scientific, Inc.) was reversed transcribed into complementary DNA (cDNA) using a cDNA Synthesis kit (Invitrogen; Thermo Fisher Scientific, Inc.) according to the manufacturer's instructions. Afterwards, qPCR was performed using SYBR Premix Ex Taq reagents (Takara Bio, Inc.) on an ABI 7500 quantitative PCR instrument (Applied Biosystems; Thermo Fisher Scientific, Inc.). The thermocycling conditions used were as follows: 95°C for 10 min, followed by 40 cycles of 95°C for 15 sec and 60°C for 1 min. The following primers were used to amplify the target genes: CBX4 forward (F), 5'-CTGGTGAAATGGAGAGGC-3' and reverse (R), 5'-GAACGACGGGCAAAGGTAGG-3'; VEGF F, 5'-ATCTTC AAGCCATCCTGTGTGC-3' and R, 5'-CAAGGCCACAG GGATTTTC-3'; VEGFR2 F, 5'-GGAACCTCACTATCCGCA GAGT-3' and R, 5'-CCAAGTTCGTCTTTTCTGGGC-3'; and GAPDH F, 5'-GCACCGTCAAGGCTGAGAAC-3' and R: 5'-ATGGTGGTGAAGACGCCAGT-3'. GAPDH served as the endogenous control and the expression levels of CBX4, VEGF and VEGFR2 were determined using the  $2^{-\Delta\Delta C_q}$  method (21).

**Western blot assay.** Total protein extracted from TPC-1 cells with the application of RIPA lysis buffer (Beyotime Institute of Biotechnology) was centrifuged at 12,000 x g for 15 min at 4°C and protein concentration was determined using the BCA method. A total of 30 µg/lane of protein samples were separated by 10% SDS-PAGE and then transferred onto PVDF membranes. After blocking in 5% non-fat milk for 1 h at 37°C, membranes were probed with primary antibodies [anti-CBX4 (1:1,000; cat. no. ab4189; Abcam), anti-NANOG (1:1,000; cat. no. ab109250; Abcam), anti-OCT4 (1:1,000; cat. no. ab19857; Abcam), anti-CD133 (1:2,000; cat. no. ab222782; Abcam), anti-MMP2 (1:1,000; cat. no. ab92536; Abcam), anti-MMP9 (1:1,000; cat. no. ab76003; Abcam), anti-E-cadherin (1:1,000; cat. no. ab40772; Abcam), anti-N-cadherin (1:5,000; cat. no. ab76011; Abcam) and anti-Vimentin (1:1,000; cat. no. ab92547; Abcam)] overnight at 4°C and subsequently incubated with HRP-conjugated secondary antibodies (1:20,000, cat. no. ab6721; Abcam) for 1 h at 37°C. Protein signals were developed using an electrochemiluminescence (ECL) kit (Beyotime Institute of Biotechnology) and protein band intensities were analyzed using Image J software (version 1.52; National Institutes of Health).

**Statistical analysis.** Data from three independent repeats were expressed as the mean ± SD. One-way analysis of variance followed by Tukey's post hoc test was employed for analyses of multiple groups and unpaired Student's t-test was employed for analyses of two groups. P<0.05 was considered to indicate a statistically significant difference.

## Results

**FMNT treatment suppresses the proliferative and clone-forming abilities of PTC cells.** FMNT is an isoflavonoid isolated from *Astragalus membranaceus* and *Spatholobus*

*suberectus* (Fig. 1A). Human TPC-1 and normal human thyroid Nthy-ori3-1 cell lines were treated with 0, 10, 30 or 100 µM FMNT, for 24 h. The CCK-8 assay revealed that FMNT treatment had no apparent influence on the viability of Nthy-ori3-1 cells while it significantly reduced the viability of TPC-1 cells in a concentration-dependent manner (Fig. 1B). The colony formation assay revealed that FMNT treatment inhibited the clone-forming ability of TPC-1 cells in a concentration-dependent manner (Fig. 1C). EdU staining demonstrated that FMNT treatment dose-dependently decreased the proportion of EdU-positive cells, which indicated that FMNT treatment repressed the proliferation of TPC-1 cells in a dose-dependent manner (Fig. 1D).

**FMNT treatment represses the migration, invasion, EMT and angiogenesis of PTC cells.** As demonstrated by the wound healing and Transwell assays, FMNT treatment suppressed the migratory and invasive capacities of TPC-1 cells in a dose-dependent manner (Fig. 2A and B). MMPs are able to degrade the extracellular matrix (ECM), facilitating the metastasis of malignant tumor (22). It was observed that FMNT treatment also dose-dependently decreased the expression levels of MMP2 and MMP9 (Fig. 2C). Tumors derive metastatic ability through EMT (23). The levels of EMT-associated biomarkers (E-cadherin, N-cadherin and Vimentin) were detected. FMNT treatment dose-dependently elevated E-cadherin expression and reduced N-cadherin and Vimentin expression levels, suppressing EMT of TPC-1 cells (Fig. 2D). Angiogenesis is important for nutritional provision in tumor growth and metastasis (24). Tube formation and angiogenesis-associated biomarkers (VEGF and VEGFR2) were detected to evaluate the angiogenesis ability of HUVECs. FMNT treatment dose-dependently inhibited tube formation and decreased VEGF and VEGFR2 levels, indicating that FMNT treatment suppressed angiogenesis in a dose-dependent manner (Fig. 2E-G). In summary, FMNT treatment could suppress PTC metastasis.

**FMNT treatment inhibits stemness characteristics of PTC cells.** Sphere formation and stemness-associated biomarkers (NANOG, OCT4 and CD133) were detected to evaluate PTC cell stemness. FMNT treatment dose-dependently inhibited sphere formation and reduced the expression levels of NANOG, OCT4 and CD133, indicating that FMNT treatment repressed the stemness of TPC-1 cells in a dose-dependent manner (Fig. 3).

**FMNT targets and downregulates CBX4 expression.** Expression of CBX4 in thyroid cancer tissues was explored using the ENCORI database (<http://rna.sysu.edu.cn/encori/mirTarPathways.php>). ENCORI data indicated that CBX4 expression was upregulated in thyroid cancer tissues in comparison with that in normal tissues (Fig. 4A). Meanwhile, differences in the expression levels of CBX4 in TPC-1 cells and Nthy-ori3-1 cells were assessed using RT-qPCR and western blot analysis. In comparison with those in Nthy-ori3-1 cells, CBX4 mRNA and protein levels were significantly upregulated in TPC-1 cells (Fig. 4B). Furthermore, molecular docking was performed to explore the compound-protein binding potential between FMNT

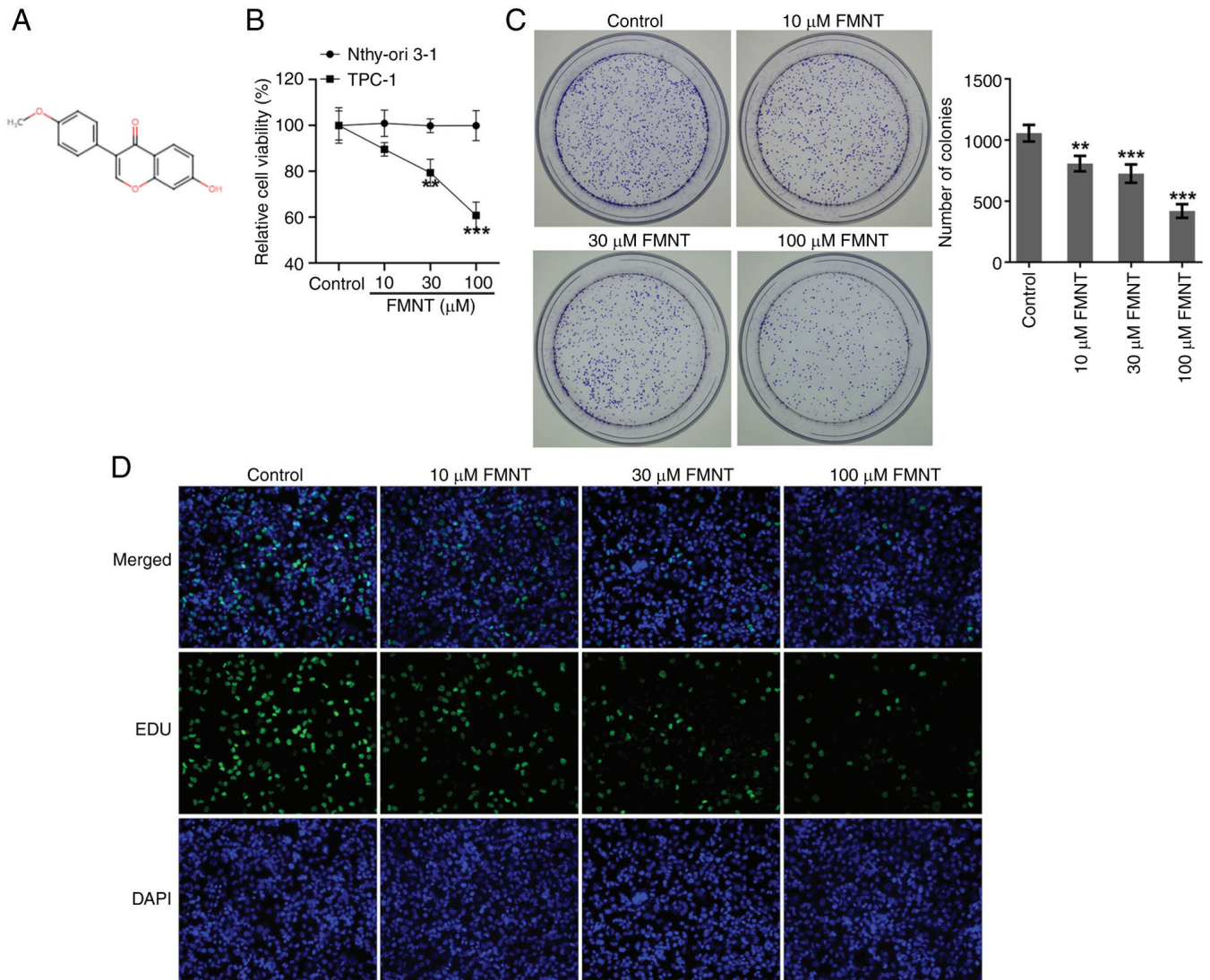


Figure 1. FMNT treatment suppresses the proliferative and clone-forming abilities of PTC cells. (A) The structure of FMNT. (B) Human PTC cell line (TPC-1) and normal human thyroid cell line (Nthy-ori3-1) were treated with 0, 10, 30 or 100 μM FMNT for 24 h. The viabilities of TPC-1 cells and Nthy-ori3-1 cells were determined by Cell Counting Kit-8 assay. The cell viability was calculated by setting the viability of the control cells as 100%. \*\*P<0.01 and \*\*\*P<0.001 vs. the Nthy-ori3-1 group. (C) TPC-1 cells were treated with 0, 10, 30 and 100 μM FMNT for 24 h. The clone-forming ability of TPC-1 cells was evaluated by colony formation assay. \*\*P<0.01 and \*\*\*P<0.001 vs. the Control group. (D) The proliferative ability of TPC-1 cells was evaluated using 5-ethynyl-2'-deoxyuridine staining (magnification, x200). FMNT, formononetin; PTC, papillary thyroid carcinoma.

and CBX4 and the result demonstrated that FMNT could interact with CBX4 at the sites of TRP:32, PHE:11, HIS:9, ASN:47 and THR:41 (Fig. 4C). Which indicated that CBX4 served as a downstream target of FMNT. Moreover, it was also demonstrated that FMNT treatment downregulated CBX4 expression in TPC-1 cells in a dose-dependent manner (Fig. 4D).

*FMNT treatment suppresses the proliferative and clone-forming abilities of PTC cells by downregulating CBX4 expression.* Whether CBX4 was involved in the anticarcinogenic effects of FMNT against PTC was further investigated. oe-CBX4 was introduced into TPC-1 cells to upregulate CBX4 expression and transfection efficacy was checked using RT-qPCR and western blot analysis (Fig. 5A). FMNT treatment significantly inhibited the clone-forming ability of TPC-1 cells, which was partially reversed by CBX4 overexpression (Fig. 5B). Upregulation of CBX4 increased

the proportion of EdU-positive cells, indicating that the suppressive effect of FMNT on the proliferation of TPC-1 cells was abolished by CBX4 overexpression (Fig. 5C). In conclusion, FMNT treatment may suppress the proliferative and clone-forming abilities of PTC cells depending on down-regulation of CBX4.

*FMNT treatment represses the migration, invasion, EMT and angiogenesis of PTC cells by downregulating CBX4 expression.* FMNT treatment significantly suppressed the migration and invasion of TPC-1 cells, which was partially reversed by CBX4 overexpression (Fig. 6A and B). Moreover, upregulation of CBX4 elevated the protein expression levels of MMP2 and MMP9, indicating that the suppressive effect of FMNT on the ECM-degrading function of MMPs was abolished by CBX4 overexpression (Fig. 6C). Upregulation of CBX4 significantly reduced E-cadherin expression and elevated N-cadherin and Vimentin expression levels, indicating that

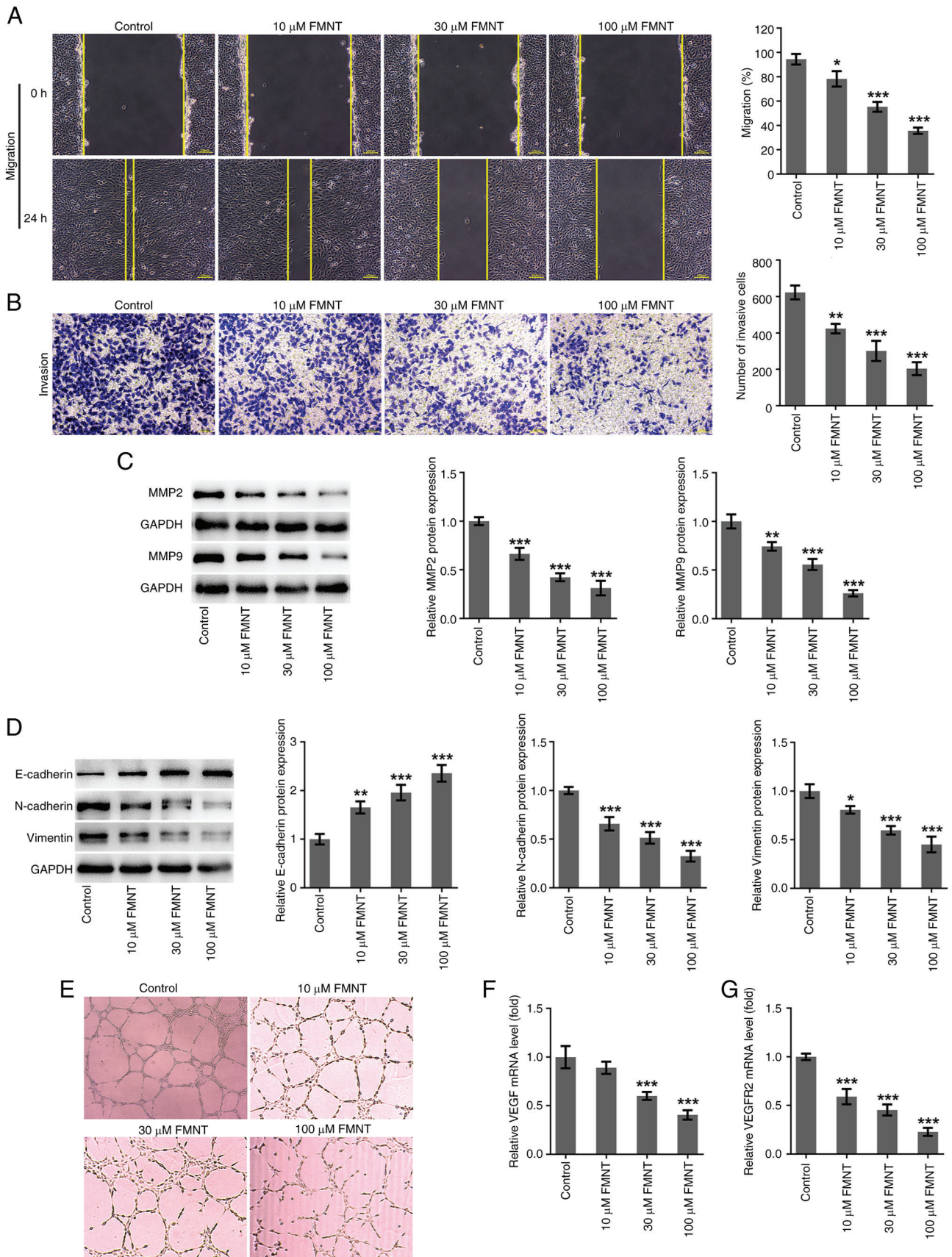


Figure 2. FMNT treatment represses the migration, invasion, EMT and angiogenesis of papillary thyroid carcinoma cells. TPC-1 cells were treated with 0, 10, 30 and 100  $\mu$ M FMNT for 24 h. (A) The migratory ability of TPC-1 cells was evaluated by wound healing assay (magnification, x100). (B) The invasive ability of TPC-1 cells was evaluated by Transwell assay (magnification, x100). (C) Expression levels of MMP2 and MMP9 in TPC-1 cells were determined by western blot analysis. (D) Expression levels of E-cadherin, N-cadherin and Vimentin in TPC-1 cells were determined by western blotting. (E) HUVECs were incubated with the conditioned media of TPC-1 cells at 37°C for 24 h. *In vitro* angiogenesis of HUVECs was evaluated using a tube formation assay (magnification, x200). (F) VEGF and (G) VEGFR2 levels in TPC-1 cells were determined by reverse transcription-quantitative PCR. \* $P < 0.05$ , \*\* $P < 0.01$  and \*\*\* $P < 0.001$  vs. the Control group. FMNT, formononetin; HUVECs, human umbilical vein endothelial cells.

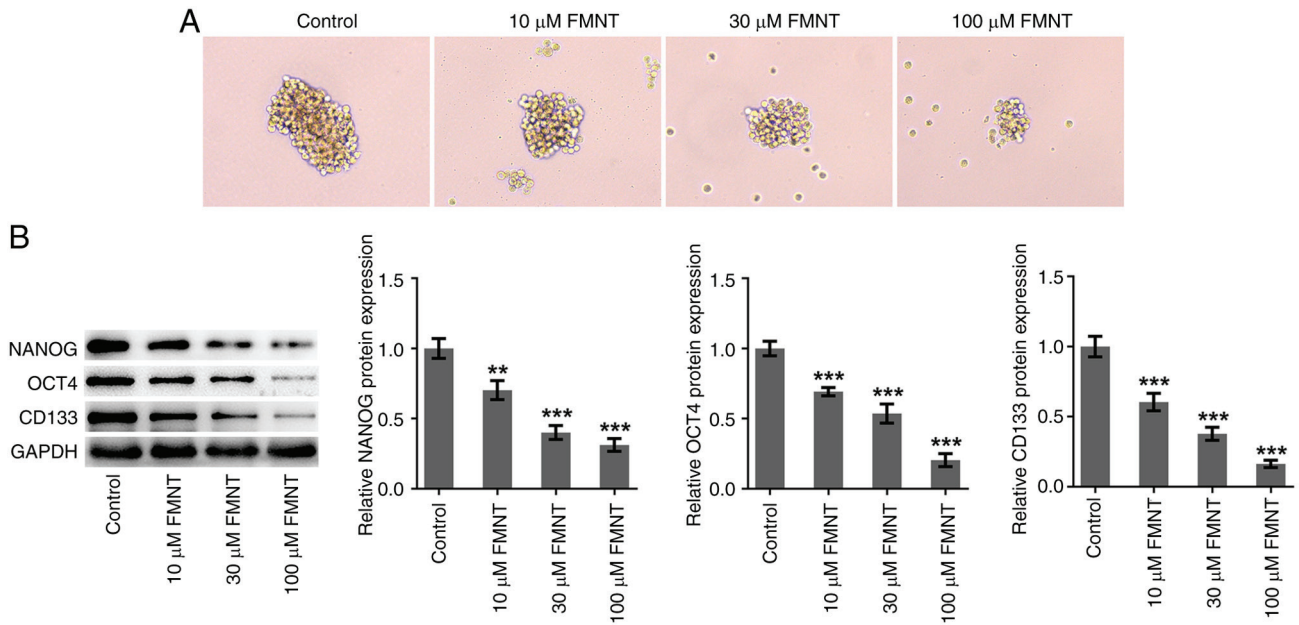


Figure 3. FMNT treatment inhibits stemness characteristics of papillary thyroid carcinoma cells. TPC-1 cells were treated with 0, 10, 30 and 100  $\mu$ M FMNT for 24 h. (A) Sphere formation of TPC-1 cells was evaluated by sphere formation assay (magnification, x200). (B) Expression levels of NANOG, OCT4 and CD133 in TPC-1 cells were determined by western blot analysis. \*\* $P < 0.01$  and \*\*\* $P < 0.001$  vs. the Control group. FMNT, formononetin.

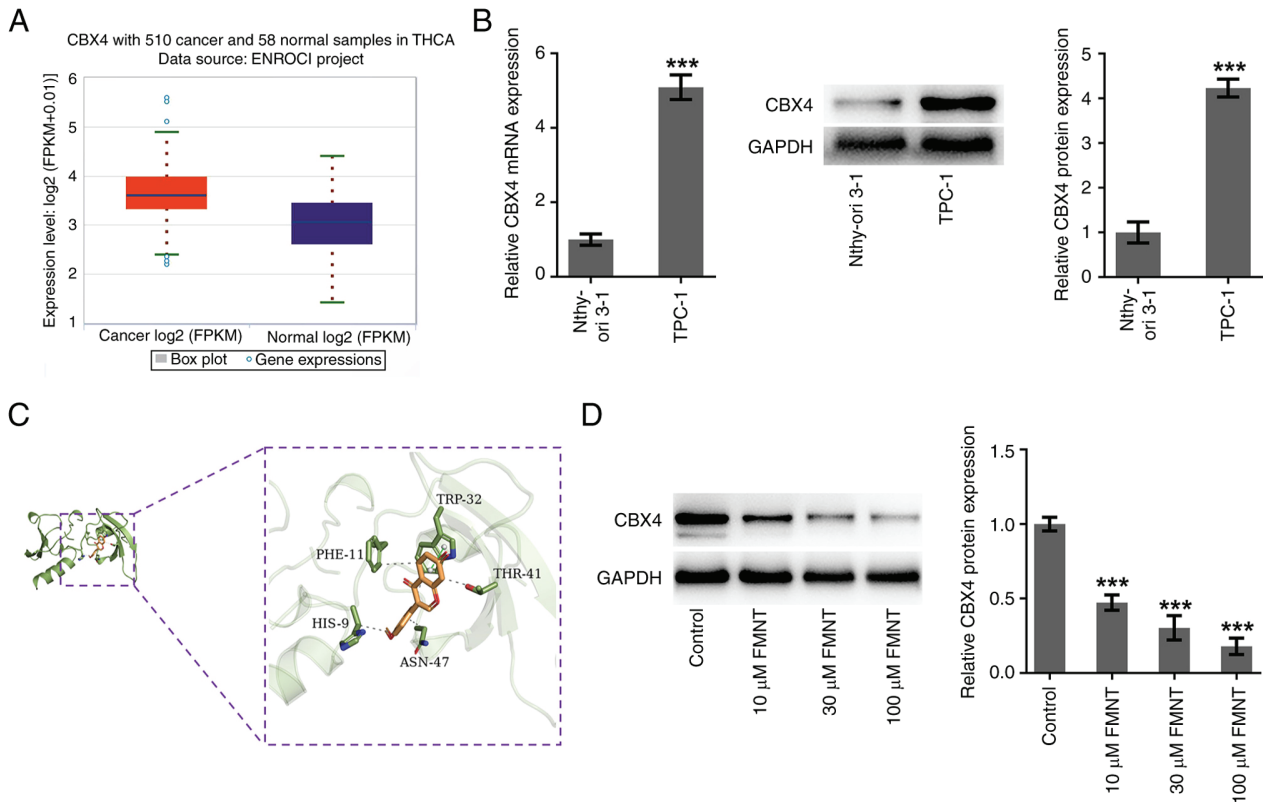


Figure 4. FMNT targets and downregulates CBX4 expression. (A) CBX4 expression levels in thyroid cancer tissues and normal tissues were obtained from the Encyclopedia of RNA Interactomes database. (B) CBX4 expression levels in TPC-1 cells and Nthy-ori3-1 cells were determined using reverse transcription-quantitative PCR and western blot analysis. \*\*\* $P < 0.001$  vs. the Nthy-ori3-1 group. (C) Molecular docking of the compound-protein interactions between FMNT and CBX4. (D) TPC-1 cells were treated with 0, 10, 30 and 100  $\mu$ M FMNT for 24 h. CBX4 expression levels in TPC-1 cells was determined by western blot analysis. \*\*\* $P < 0.001$  vs. the Control group. FMNT, formononetin; CBX4, chromobox homolog 4.

the suppressive effect of FMNT on EMT was abolished by CBX4 overexpression (Fig. 6D). In addition, FMNT treatment inhibited tube formation and significantly decreased

VEGF and VEGFR2 mRNA expression levels, which was partially reversed by CBX4 overexpression (Fig. 6E-G). Upregulation of CBX4 abolished the suppressive effect of

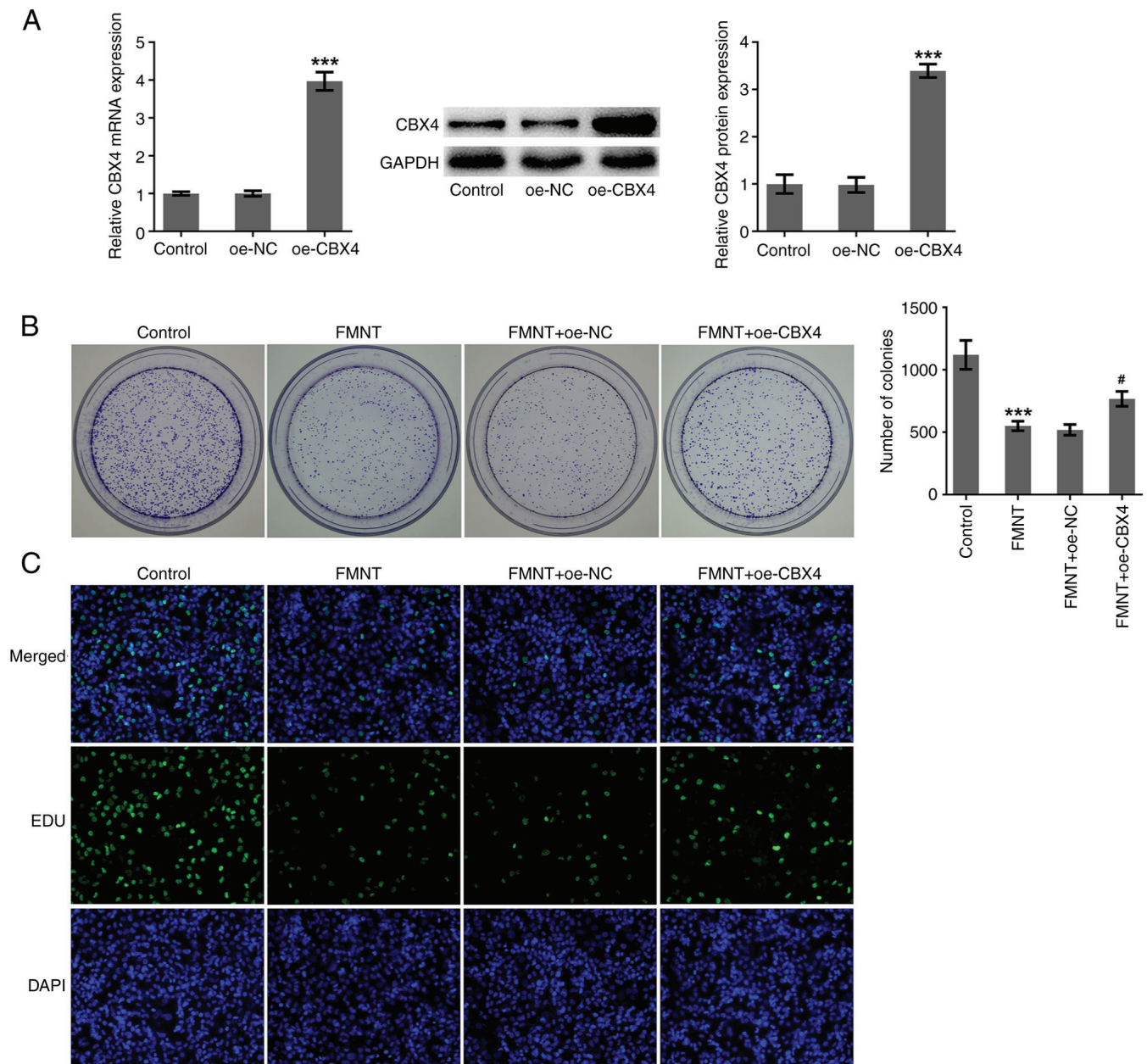


Figure 5. FMNT treatment suppresses the proliferative and clone-forming abilities of papillary thyroid carcinoma cells by downregulating CBX4 expression. (A) TPC-1 cells were transfected with oe-CBX4 or oe-NC. CBX4 expression in TPC-1 cells was determined by reverse transcription-quantitative PCR and western blot analysis. \*\*\* $P < 0.001$  vs. oe-NC. (B) FMNT-treated TPC-1 cells were transfected with oe-CBX4 or oe-NC. The clone-forming ability of TPC-1 cells was evaluated using a colony formation assay. \*\*\* $P < 0.001$  vs. the Control group; # $P < 0.05$  vs. FMNT + oe-NC. (C) FMNT-treated TPC-1 cells were transfected with oe-CBX4 or oe-NC. The proliferative ability of TPC-1 cells was evaluated using EdU staining (magnification, x200). FMNT, formononetin; CBX4, chromobox homolog 4; oe, overexpression; NC, negative control.

FMNT on angiogenesis. In summary, FMNT treatment may repress PTC metastasis depending on downregulation of CBX4.

*FMNT treatment inhibits stemness characteristics of PTC cells by downregulating CBX4 expression.* FMNT treatment inhibited sphere formation and significantly reduced the protein expression levels of NANOG, OCT4 and CD133, which was partially reversed by CBX4 overexpression (Fig. 7). Upregulation of CBX4 abolished the suppressive effect of FMNT on PTC cell stemness. In conclusion, FMNT treatment may inhibit the stemness characteristics of PTC cells depending on downregulation of CBX4.

## Discussion

Although the treatment options available for PTC diagnosed at an early stage are effective and achieve comparatively improved prognosis and clinical outcome in comparison with those for metastasized and relapsed forms of PTC, there are more challenges in treating metastasized and relapsed forms of PTC (25). The present study investigated the anticarcinogenic effects of FMNT in the malignant progression of PTC as well as identifying the intrinsic molecular mechanism. Based on the preliminary results, FMNT was innovatively described by the authors as an anti-tumorigenic agent in PTC via downregulation of CBX4.

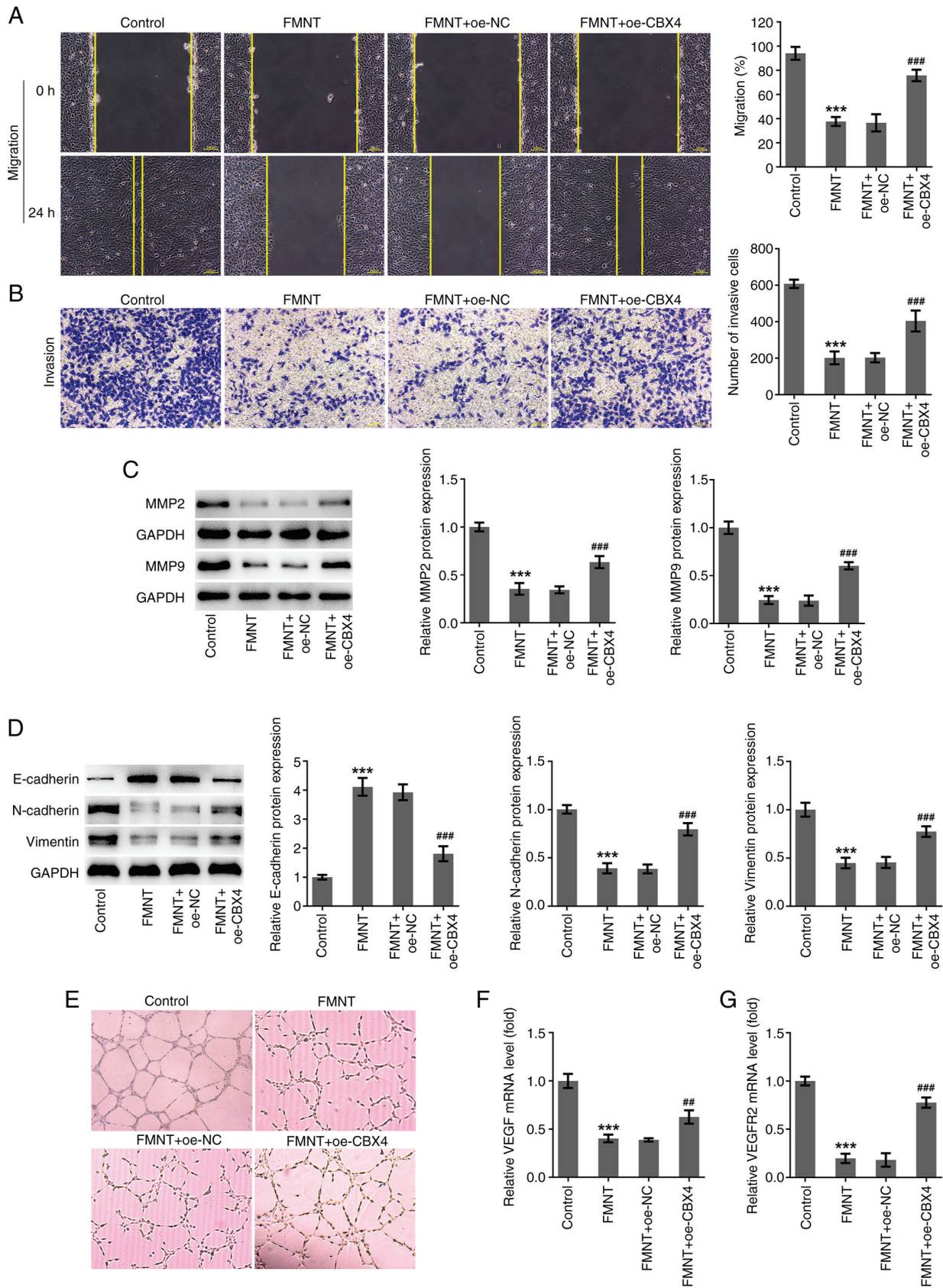


Figure 6. FMNT treatment represses the migration, invasion, EMT and angiogenesis of papillary thyroid carcinoma cells by downregulating CBX4 expression. FMNT-treated TPC-1 cells were transfected with oe-CBX4 or oe-NC. (A) The migratory ability of TPC-1 cells was evaluated by wound healing assay (magnification, x100). (B) The invasive ability of TPC-1 cells was evaluated using a Transwell assay (magnification, x100). (C) Expression levels of MMP2 and MMP9 in TPC-1 cells were determined by western blotting. (D) Expression levels of E-cadherin, N-cadherin and Vimentin in TPC-1 cells were determined by western blot analysis. (E) HUVECs were incubated with the CM of TPC-1 cells at 37°C for 24 h. *In vitro* angiogenesis of HUVECs was evaluated by tube formation assay (magnification, x200). (F and G) VEGF and VEGFR2 levels in TPC-1 cells were determined by reverse transcription-quantitative PCR. \*\*\*P<0.001 vs. the Control group; \*\*P<0.01 and ###P<0.001 vs. FMNT+oe-NC. FMNT, formononetin; CBX4, chromobox homolog 4; oe, overexpression; NC, negative control; HUVECs, human umbilical vein endothelial cells.



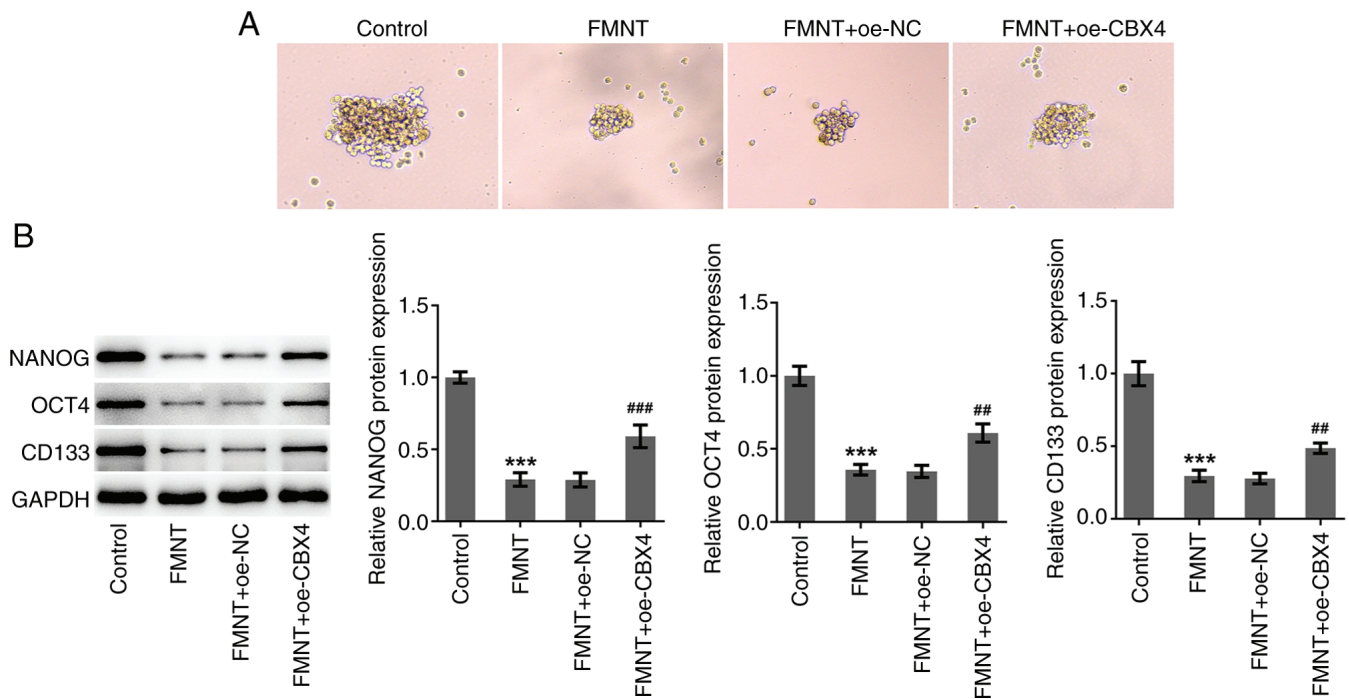


Figure 7. FMNT treatment inhibits stemness characteristics of papillary thyroid carcinoma cells by downregulating CBX4 expression. FMNT-treated TPC-1 cells were transfected with oe-CBX4 or oe-NC. (A) Sphere formation of TPC-1 cells was evaluated by sphere formation assay (magnification, x200). (B) Expression levels of NANOG, OCT4 and CD133 in TPC-1 cells were determined by western blot analysis. \*\*\*P<0.001 vs. the Control group; \*\*P<0.01 and ###P<0.001 vs. FMNT + oe-NC. FMNT, formononetin; CBX4, chromobox homolog 4; oe, overexpression; NC, negative control.

The combinational use of FMNT and metformin can induce cell growth inhibition and apoptosis of breast cancer cells by mediating the ERK1/2 signaling pathway (6). FMNT can impair the proliferative, migratory and invasive capabilities of human breast cancer cells via blockade of PI3K/Akt signaling (7,8). FMNT can exert anti-colorectal cancer effects through suppression of cellular proliferation and regulation of cancer-related metabolic pathways (9). FMNT can inhibit the growth and aggressiveness of gastric cancer cells *in vitro* and *in vivo* by downregulating microRNA (miR)-542-5p expression (10). Novel hybrids of FMNT and podophyllotoxin can suppress the growth, migration and invasion of lung cancer cells (11). In the present study, it was demonstrated that FMNT suppressed the proliferation, clone formation, migration, invasion, EMT, angiogenesis and stemness of PTC cells.

Higher expression levels of CBX4 in thyroid cancer tissues were assessed using the ENCOR1 database. In the present study, it was also demonstrated that CBX4 was highly expressed in human PTC cell line TPC-1 in comparison with normal human thyroid cell line Nthy-ori3-1. Importantly, molecular docking confirmed the compound-protein binding potential between FMNT and CBX4. The binding stability of FMNT and CBX4 was enhanced by five hydrophobic interactions, observed at TRP:32, PHE:11, HIS:9, ASN:47 and THR:41. In addition, FMNT formed hydrophobic interactions by  $\pi$ - $\pi$  stacking at the active site residues with TRP:32. Therefore, the inhibition of CBX4 by FMNT might be attributed to this unique binding pattern. Additionally, it was shown that FMNT treatment dose-dependently downregulated CBX4 expression in TPC-1 cells. Based on the aforementioned results, it was hypothesized that the anticarcinogenic effects of FMNT against PTC may be implicated in suppression of CBX4. In hepatocellular

carcinoma patients, CBX4 expression is closely associated with tumor size and pathologic differentiation and patients who have a higher level of CBX4 in cytoplasm suffer from a shorter overall survival and recurrence-free survival (16). CBX4 can promote proliferation and metastasis via regulation of BMI-1 in lung cancer (17). CBX4 can promote gastric cancer progression and stemness via activating CDC20 (26). CBX4 can transcriptionally suppress KLF6 via interaction with HDAC1 to exert oncogenic activities in clear cell renal cell carcinoma (19). CBX4 overexpression can reverse the suppressive effects of miR-515-5p on the proliferation, migration and invasion of human breast cancer cells (20). In the present study, it was demonstrated that upregulation of CBX4 partially abolished the suppressive effects of FMNT on the proliferation, clone formation, migration, invasion, EMT, angiogenesis and stemness of PTC cells. In view of the aforementioned results, it was hypothesized that FMNT might exert antitumor activity in PTC through multiple-target therapy rather than single-target therapy. Molecular docking also demonstrated the compound-protein binding potential between FMNT and stabilin-2 (SATB2), FMNT and estrogen receptor  $\alpha$  (ESR1). SATB2 and ESR1 have been considered as the potential oncogenes. Whether the anticarcinogenic effects of FMNT against PTC are implicated in suppression of SATB2 and ESR1 will be the highlights in the following research.

Collectively, FMNT can act as an anti-tumorigenic agent in PTC via suppression of CBX4. The results of the present study are beneficial to the development of promising agents and effective therapeutic targets for PTC. The current study has certain limitations; only the TCP-1 cell line derived from male PTC patients was used. Considering that the absolute number of female PTC patients is more than twice that of male PTC

patients, presents a limitation to use of these results. In future studies, another cell line derived from female PTC patients should be further examined to enhance the persuasiveness of the conclusions in the present research. Moreover, clinical analysis should be conducted in the future to support the present findings and to excavate the predictive values of FMNT.

### Acknowledgements

Not applicable.

### Funding

No funding was received.

### Availability of data and materials

The data generated in the present study may be requested from the corresponding author.

### Authors' contributions

HY contributed to the conception, study design, experimental operation, manuscript writing and critical review. JQ contributed to experimental operation, data collection, data analysis and manuscript writing. HG contributed to experimental operation, data collection and manuscript writing. YZ contributed to the conception, study design, manuscript writing and critical revision. All authors read and approved the final version of the manuscript. HY and YZ confirm the authenticity of all the raw data.

### Ethics approval and consent to participate

Not applicable.

### Patient consent for publication

Not applicable.

### Competing interests

The authors declare that they have no competing interests.

### References

- Siegel RL, Miller KD and Jemal A: Cancer statistics, 2016. *CA Cancer J Clin* 66: 7-30, 2016.
- Zhang W, Ruan X, Li Y, Zhi J, Hu L, Hou X, Shi X, Wang X, Wang J, Ma W, *et al.*: KDM1A promotes thyroid cancer progression and maintains stemness through the Wnt/ $\beta$ -catenin signaling pathway. *Theranostics* 12: 1500-1517, 2022.
- Haugen BR, Alexander EK, Bible KC, Doherty GM, Mandel SJ, Nikiforov YE, Pacini F, Randolph GW, Sawka AM, Schlumberger M, *et al.*: 2015 American thyroid association management guidelines for adult patients with thyroid nodules and differentiated thyroid cancer: The American thyroid association guidelines task force on thyroid nodules and differentiated thyroid cancer. *Thyroid* 26: 1-133, 2016.
- Davies L and Welch HG: Current thyroid cancer trends in the United States. *JAMA Otolaryngol Head Neck Surg* 140: 317-322, 2014.
- Jiang D, Rasul A, Batool R, Sarfraz I, Hussain G, Mateen Tahir M, Qin T, Selamoglu Z, Ali M, Li J and Li X: Potential anticancer properties and mechanisms of action of formononetin. *Biomed Res Int* 2019: 5854315, 2019.
- Xin M, Wang Y, Ren Q and Guo Y: Formononetin and metformin act synergistically to inhibit growth of MCF-7 breast cancer cells in vitro. *Biomed Pharmacother* 109: 2084-2089, 2019.
- Chen J, Zeng J, Xin M, Huang W and Chen X: Formononetin induces cell cycle arrest of human breast cancer cells via IGF1/PI3K/Akt pathways in vitro and in vivo. *Horm Metab Res* 43: 681-686, 2011.
- Zhou R, Xu L, Ye M, Liao M, Du H and Chen H: Formononetin inhibits migration and invasion of MDA-MB-231 and 4T1 breast cancer cells by suppressing MMP-2 and MMP-9 through PI3K/AKT signaling pathways. *Horm Metab Res* 46: 753-760, 2014.
- Zhang L, Gong Y, Wang S and Gao F: Anti-colorectal cancer mechanisms of formononetin identified by network pharmacological approach. *Med Sci Monit* 25: 7709-7714, 2019.
- Wang WS and Zhao CS: Formononetin exhibits anticancer activity in gastric carcinoma cell and regulating miR-542-5p. *Kaohsiung J Med Sci* 37: 215-225, 2021.
- Yang C, Xie Q, Zeng X, Tao N, Xu Y, Chen Y, Wang J and Zhang L: Novel hybrids of podophyllotoxin and formononetin inhibit the growth, migration and invasion of lung cancer cells. *Bioorg Chem* 85: 445-454, 2019.
- Chan HL and Morey L: Emerging Roles for polycomb-group proteins in stem cells and cancer. *Trends Biochem Sci* 44: 688-700, 2019.
- Klauke K, Radulović V, Broekhuis M, Weersing E, Zwart E, Olthof S, Ritsema M, Bruggeman S, Wu X, Helin K, *et al.*: Polycomb Cbx family members mediate the balance between haematopoietic stem cell self-renewal and differentiation. *Nat Cell Biol* 15: 353-362, 2013.
- Ismail IH, Gagné JP, Caron MC, McDonald D, Xu Z, Masson JY, Poirier GG and Hendzel MJ: CBX4-mediated SUMO modification regulates BMI1 recruitment at sites of DNA damage. *Nucleic Acids Res* 40: 5497-5510, 2012.
- Pan Y, Li Q, Cao Z and Zhao S: The SUMO E3 ligase CBX4 is identified as a poor prognostic marker of gastric cancer through multipronged OMIC analyses. *Genes Dis* 8: 827-837, 2021.
- Wang B, Tang J, Liao D, Wang G, Zhang M, Sang Y, Cao J, Wu Y, Zhang R, Li S, *et al.*: Chromobox homolog 4 is correlated with prognosis and tumor cell growth in hepatocellular carcinoma. *Ann Surg Oncol* 20 (Suppl 3): S684-S692, 2013.
- Hu C, Zhang Q, Tang Q, Zhou H, Liu W, Huang J, Liu Y, Wang Q, Zhang J, Zhou M, *et al.*: CBX4 promotes the proliferation and metastasis via regulating BMI-1 in lung cancer. *J Cell Mol Med* 24: 618-631, 2020.
- Fang X and Pan A: MiR-507 inhibits the progression of gastric carcinoma via targeting CBX4-mediated activation of Wnt/ $\beta$ -catenin and HIF-1 $\alpha$  pathways. *Clin Transl Oncol* 24: 2021-2028, 2022.
- Jiang N, Niu G, Pan YH, Pan W, Zhang MF, Zhang CZ and Shen H: CBX4 transcriptionally suppresses KLF6 via interaction with HDAC1 to exert oncogenic activities in clear cell renal cell carcinoma. *EBioMedicine* 53: 102692, 2020.
- Wen LJ, Wang YS and Tan PY: miR-515-5p inhibits the proliferation, migration and invasion of human breast cancer cells by targeting CBX4. *Exp Ther Med* 22: 1328, 2021.
- Livak KJ and Schmittgen TD: Analysis of relative gene expression data using real-time quantitative PCR and the 2(-Delta Delta C(T)) method. *Methods* 25: 402-408, 2001.
- Winer A, Adams S and Mignatti P: Matrix metalloproteinase inhibitors in cancer therapy: Turning past failures into future successes. *Mol Cancer Ther* 17: 1147-1155, 2018.
- Aiello NM and Kang Y: Context-dependent EMT programs in cancer metastasis. *J Exp Med* 216: 1016-1026, 2019.
- Paduch R: The role of lymphangiogenesis and angiogenesis in tumor metastasis. *Cell Oncol (Dordr)* 39: 397-410, 2016.
- Khan AQ, Ahmed EI, Elareer N, Fathima H, Prabhu KS, Siveen KS, Kulinski M, Azizi F, Dermime S, Ahmad A, *et al.*: Curcumin-mediated apoptotic cell death in papillary thyroid cancer and cancer stem-like cells through targeting of the JAK/STAT3 signaling pathway. *Int J Mol Sci* 21: 438, 2020.
- Li W, Chen H, Wang Z, Liu J, Lei X and Chen W: Chromobox 4 (CBX4) promotes tumor progression and stemness via activating CDC20 in gastric cancer. *J Gastrointest Oncol* 13: 1058-1072, 2022.

